

N-BODY GROWTH OF A BAHCALL-WOLF CUSP AROUND A BLACK HOLE

MIGUEL PRETO

Department of Physics and Astronomy, Rutgers University, New Brunswick, NJ 08903, USA

DAVID MERRITT

Department of Physics, Rochester Institute of Technology, Rochester, NY 14623, USA

AND

RAINER SPURZEM

Astronomisches Rechen-Institut Heidelberg, Mönchhofstrasse 12–14, 69120 Heidelberg, Germany

Draft version 14th May 2021

Abstract

We present a clear N -body realization of the growth of a Bahcall-Wolf $f \propto E^{1/4}$ ($\rho \propto r^{-7/4}$) density cusp around a massive object (“black hole”) at the center of a stellar system. Our N -body algorithm incorporates a novel implementation of Mikkola-Aarseth chain regularization to handle close interactions between star and black hole particles. Forces outside the chain were integrated on a GRAPE-6A/8 special-purpose computer with particle numbers up to $N = 0.25 \times 10^6$. We compare our N -body results with predictions of the isotropic Fokker-Planck equation and verify that the time dependence of the density (both configuration and phase-space) predicted by the Fokker-Planck equation is well reproduced by the N -body algorithm, for various choices of N and of the black hole mass. Our results demonstrate the feasibility of direct-force integration techniques for simulating the evolution of galactic nuclei on relaxation time scales.

Subject headings: stellar dynamics, galaxies: nuclei, black holes

1. INTRODUCTION

The distribution of stars around a massive black hole is a classic problem in galactic dynamics. Many such distributions are possible, depending on the initial state, the mode of formation of the black hole, and the time since its formation. However, a number of plausible scenarios predict a steeply-rising stellar density within the black hole’s sphere of influence, $r \lesssim r_h \equiv GM_{BH}/\sigma^2$, with M_{BH} the black hole mass and σ^2 the 1D stellar velocity dispersion outside of r_h . Such models receive support from the observed run of stellar density with radius near the centers of the nearest galaxies known to contain massive black holes: the Milky Way, M31 and M32. The nucleus of each galaxy has a density cusp with $\rho \sim r^{-\gamma}$, $\gamma \approx 1.5$ within the black hole’s sphere of influence (Lauer et al. 1998; Genzel et al. 2003). This is consistent with the slope predicted by so-called adiabatic growth models, in which a black hole with small initial mass is embedded in a star cluster and its mass increased to some final value, on a time scale long compared with orbital periods. The final density in the adiabatic growth model follows a power law at $r \lesssim r_h$, with index γ_f that depends on the initial stellar distribution function. If the initial model is a non-singular isothermal sphere, then $\gamma_f = 3/2$ (Peebles 1972a; Young 1980). However a non-singular isothermal sphere seems a rather ad hoc guess for the initial state, and initial models without flat cores give steeper final slopes, $1.5 \lesssim \gamma_f \lesssim 2.5$ (Merritt 2004).

Uncertainties in the initial state are less consequential if the stellar cluster is old compared with the time T_r for gravitational scattering to redistribute energy between stars. In this case, one expects the collisional transport of mass and energy to set up a steady-state distribution whose functional form is independent of the initial phase-space density. Peebles (1972b) first addressed this problem and derived a power-law index $\gamma = 9/4$ for the stellar density within r_h . Peebles obtained his solution by setting the flux of stars in energy space to a con-

stant non-zero value. Shapiro & Lightman (1976) and Bahcall & Wolf (1976) criticized the Peebles derivation on the grounds that the implied flux is unphysically large, in fact divergent if the solution is extended all the way to the black hole. A physically more reasonable solution would have a nearly zero flux of stars into the black hole. Bahcall & Wolf (1976) repeated Peebles’s derivation, setting the phase-space density $f(E)$ to zero at the black hole’s tidal disruption radius. They found that f evolves, in a time only slightly longer than T_r , to a steady state in which the flux is close to zero at all energies. The zero-flux solution has $f \propto E^{1/4}$ within the black hole’s sphere of influence, with $E \geq 0$ the binding energy; the corresponding stellar density is $\rho \propto r^{-7/4}$.

The Bahcall-Wolf solution has been verified in a number of subsequent studies, almost all of which were based on the Fokker-Planck formalism (Cohn & Kulsrud 1978; Marchant & Shapiro 1980; Freitag & Benz 2002; Amaro-Seoane, Freitag & Spurzem 2004). The $f \propto E^{1/4}$ and $\rho \propto r^{-7/4}$ character of the solution has been found to be robust, at least at radii where the capture or destruction of stars occurs in a time long compared with orbital periods. But verifying the Bahcall-Wolf solution in an N -body integration is also clearly desirable, since an N -body simulation is free of many of the simplifying assumptions that limit the applicability of the Fokker-Planck equation, including the restriction to small-angle scattering, and the neglect of spatial inhomogeneities in the derivation of the diffusion coefficients. But the N -body approach is challenging: large particle numbers are required to resolve the cusp, and accurate integration schemes are needed to follow the motion of stars near the black hole.

In this paper we combine a sophisticated N -body code with the special-purpose GRAPE hardware and show that the formation of a Bahcall-Wolf cusp can be convincingly reproduced without any of the approximations that go into the

Fokker-Planck formalism. Our results provide a clear demonstration of the applicability of direct-force N -body techniques to the collisional evolution of dense star clusters, and highlight the usefulness of direct N -body techniques for understanding the dynamical evolution of galactic nuclei containing supermassive black holes.

2. METHOD

Our N -body algorithm is an adaptation of NBODY1 (Aarseth 1999) to the GRAPE-6 special-purpose hardware. Forces for the majority of the particles were computed via a direct-summation scheme without regularization. Particle positions were advanced using a fourth-order Hermite integration scheme with individual, adaptive, block time steps (Aarseth 2003). Time steps of stars near the central massive particle (“black hole”) would become prohibitively small in such a scheme. Therefore, the motion of stars near the black hole was treated via the chain regularization algorithm of Mikkola and Aarseth (Mikkola & Aarseth 1990, 1993). This scheme selects an ordering for the n particles in the chain and then regularizes the $n - 1$ pairwise interactions according to the standard Kustaanheimo-Stiefel (KS) transformation (Kustaanheimo & Stiefel 1965), such that motion in Cartesian space with a singular potential is transformed into harmonic motion in a 4D vector space.

Our chain method differs from the standard one (which is incorporated in NBODY5 and NBODY6) in two ways. First, the massive body was always positioned at the bottom of the chain; and second, the chain was ordered according to force, not distance. The chain subsystem typically consisted of the black hole plus a small number of stars, $n - 1 \approx 10 - 20$. The chain’s center of mass was a pseudo-particle as seen by the N -body code, and was advanced by the Hermite scheme in the same way as an ordinary particle. However the structure of the chain (i.e. the forces from individual chain members) was resolved as necessary for the accurate integration of nearby particles. Furthermore the equations of motion of particles within the chain included forces exerted by a list of external perturbers. Whether a given star was listed as a perturber was determined by a tidal criterion, with typically $\lesssim 10^2$ particles satisfying the criterion. Particles were denoted perturbers if their distance r to the chain center of mass satisfied $r < R_{\text{crit1}} = (m/m_{\text{ch}})^{1/3} \gamma_{\text{min}}^{-1/3} R_{\text{ch}}$, where m_{ch} and R_{ch} represent the mass and spatial size respectively of the chain, m is the mass of one star, and γ_{min} was chosen to be 10^{-6} ; thus $R_{\text{crit1}} \approx 10^2 (m/m_{\text{ch}})^{1/3} R_{\text{ch}}$. The chain was resolved for stars within a distance $R_{\text{crit2}} = \lambda_p R_{\text{ch}}$ from the chain’s center of mass, where $\lambda_p = 100$. In the standard chain implementations in NBODY5 and NBODY6 (with particles of nearly equal mass), $R_{\text{crit1}} \approx R_{\text{crit2}}$, while in our application these two radii are significantly different.

The Mikkola-Aarseth chain algorithm becomes ill-behaved in the case of extreme mass ratios between the particles, $M_{\text{BH}}/m \gtrsim 10^6$ (S. Mikkola, private communication). Aarseth (2003) advocates a time-transformed leap frog (TTL) to treat such extreme mass ratios. The largest mass ratio in our simulations is $\sim 10^3$ for which the standard chain algorithm works perfectly well. Using a minimum tolerance of 10^{-12} for the chain’s Bulirsch-Stoer integrator allowed us to reach typical relative accuracies of 10^{-9} .

3. INITIAL CONDITIONS

A crucial element of our method is the use of initial conditions that represent a precise steady state of the collision-

	γ	N	M_{BH}/m	M_{BH}/M	r_h	$\ln\Lambda$	T_r	$T_{\text{max}} (T_{\text{max}}/T_r)$
1	1/2	250K	2500	0.01	0.26	8.0	1690	1500 (0.887)
2	1/2	100K	500	0.005	0.19	6.6	454	500 (1.101)
3	1/2	100K	1000	0.01	0.26	7.1	764	800 (1.047)
4	1	100K	1000	0.01	0.17	6.6	227	200 (0.881)
5	1/2	150K	1500	0.01	0.26	7.5	1034	860 (0.832)

less Boltzmann equation. Embedding or growing a massive particle in a pre-existing stellar system can easily result in the formation of a density cusp with slope similar to that predicted by Bahcall and Wolf (1976), but for reasons having nothing to do with collisional relaxation. For instance, as discussed above, adiabatic growth of a black hole produces a density profile within the hole’s sphere of influence of $\rho \sim r^{-\gamma_{\text{sp}}}$, $1.5 \lesssim \gamma_{\text{sp}} \lesssim 2.5$; hence a cusp that forms collisionlessly can easily mimic a $\rho \propto r^{-7/4}$ collisional cusp. To avoid any possibility of non-collisional cusp formation in our simulations, which would seriously compromise the interpretation, we generated initial coordinates and velocities from the steady-state phase space density $f(E)$ that reproduces the Dehnen (1993) density law in the gravitational potential including both the stars and the black hole. The Dehnen model density satisfies $\rho(r) \propto r^{-\gamma}$ at small radii, and the $f(E)$ that reproduces Dehnen’s $\rho(r)$ in the presence of a central point mass is non-negative for all $\gamma \geq 0.5$; hence $\gamma = 0.5$ is the flattest central profile that can be adopted if the initial conditions are to represent a precise steady state. As shown in Table 1, most of our runs used initial conditions with this minimum value of γ . Henceforth we adopt units such that the gravitational constant G , the total stellar mass M , and the Dehnen scale length a are equal to one.

Table 1 also gives the other important parameters of the N -body integrations. The influence radius of the black hole r_h was defined as the radius at which the enclosed stellar mass at $t = 0$ was equal to twice the black hole mass. (This is equivalent to the more standard definition $r_h = GM_{\text{BH}}/\sigma^2$ when $\rho \propto r^{-2}$.) The relaxation time T_r was computed at $t = 0$, $r = r_h$ from the standard expression (eq. 2-62 of Spitzer 1987), setting $\ln\Lambda = \ln(r_h\sigma^2/2Gm)$. This definition of Λ is equivalent to equating b_{max} , the maximum impact parameter for encounters in Chandrasekhar’s theory, with r_h . This choice is motivated by the expectation that b_{max} for stars near the center of strongly inhomogeneous stellar system should be of order the radius at which the density falloff begins to abate, e.g. the core radius if there is a core (Maoz 1993; Merritt 2001). In our simulations, this radius is of order the Dehnen scale length $a \approx$ a few $\times r_h$ at $t = 0$, decreasing to a fraction of r_h after formation of the collisional cusp; hence a choice of $b_{\text{max}} \approx r_h$ seems appropriate. We stress that Chandrasekhar’s $\ln\Lambda$ is a poorly-defined quantity in strongly inhomogeneous and evolving systems, and our choice is at best approximate. Nevertheless, we will see that the time scaling determined by this choice of $\ln\Lambda$ results in very good correspondence between the evolution rates seen in the N -body and Fokker-Planck models.

4. FOKKER-PLANCK MODELS

We compared the N -body evolution with the predictions of the time-dependent, orbit-averaged, isotropic Fokker-Planck

equation:

$$4\pi^2 p(E) \frac{\partial f}{\partial t} = -\frac{\partial F_E}{\partial E}, \quad (1a)$$

$$F_E(E, t) = -D_{EE} \frac{\partial f}{\partial E} - D_E f, \quad (1b)$$

$$D_{EE}(E) = 64\pi^4 G^2 m^2 \ln \Lambda \times \left[q(E) \int_{-\infty}^E dE' f(E') + \int_E^{\infty} dE' q(E') f(E') \right],$$

$$D_E(E) = -64\pi^4 G^2 m^2 \ln \Lambda \int_E^{\infty} dE' p(E') f(E') \quad (1c)$$

(e.g. Cohn 1980; Spitzer 1987). Here $p(E) = 4\sqrt{2} \int_0^{r_{\max}(E)} r^2 \sqrt{E - \Phi(r)} dr = -\partial q / \partial E$ is the phase space volume accessible per unit of energy, the upper integration limit is determined via $-\Phi(r_{\max}) = E$, and $E = -v^2/2 - \Phi(r) \geq 0$ is the binding energy per unit mass (hereinafter the “energy.”) Since the gravitational potential changes as the stellar distribution evolves, equation (1) should also contain a term describing the adjustment in f due to changes in E as the gravitational potential evolves (e.g. Spitzer 1987, eq. 2-86). However changes in $\rho(r)$ only take place well within r_h in our simulations, and the potential is dominated by the (fixed) mass of the black hole in this region. Hence, assuming a fixed potential in the Fokker-Planck equation is an excellent approximation for our purposes.

When scaling the Fokker-Planck results to the N -body results, the only free parameter is $\ln \Lambda$. We used the values given in Table 1.

5. RESULTS

As the cusp develops, the density of stars at $r \lesssim r_h$ increases. This is illustrated in Figure 1, which shows the mass in stars within a radial distance $0.1r_h$ from the black hole as a function of time for each of the runs. (Distances were defined with respect to the instantaneous position of the black hole particle; the latter wanders like a Brownian particle, but the density peak tends to remain centered on the black hole as it moves.) For comparison, we also show in Figure 1 the same quantity as computed from the Fokker-Planck equation. The time scaling of the Fokker-Planck equation was set using the value of $\ln \Lambda$ given in Table 1 – no adjustments were made to optimize the fit. (We note that integrations like these could in principle be used to *evaluate* $\ln \Lambda$.) While there are hints of systematic differences in some of the runs, overall the correspondence is very good: clearly, the N -body evolution is quite close to what is predicted from the Fokker-Planck equation.

The N -body runs in Figure 1 exhibit a range in N from 0.25×10^6 (Run 1) to 0.1×10^6 (Runs 2-4), showing that the correspondence between N -body and Fokker-Planck results remains good over at least a modest range in particle number. Figure 1 also suggests that each of the integrations has reached an approximate steady state with regard to changes in the density at the final time step.

Having demonstrated the reliability of the time scaling of the Fokker-Planck equation, we can make a more detailed comparison with the N -body models. Figure 2 shows the evolution of the stellar density $\rho(r)$ in Run 1 compared with the Fokker-Planck prediction. The N -body density was computed from snapshots of the particle positions (no time averaging) using MAPEL, a maximum penalized likelihood algorithm (Merritt 1994; Merritt & Tremblay 1994). The radial coordinate was defined again as distance from the black hole. The

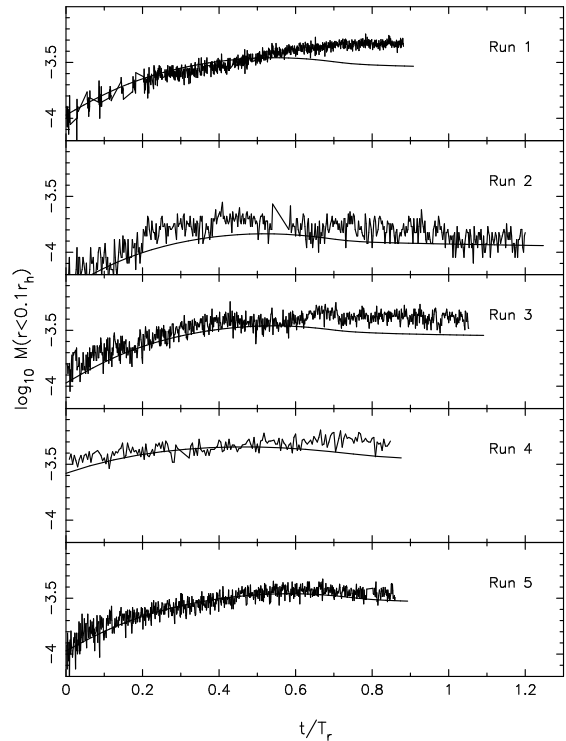


FIG. 1.— Evolution of the mass in stars within a distance $0.1r_h$ from the black hole, where r_h is the influence radius of the black hole measured at time zero. Noisy curves are from the N -body runs; smooth curves are solutions to the Fokker-Planck equation.

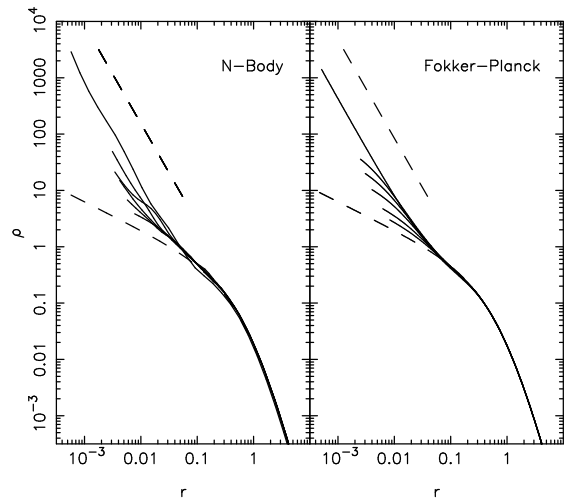


FIG. 2.— Evolution of the mass density profile around the black hole. Left panel: N -body; $\rho(r)$ was estimated from the particle positions at times $t = 100, 200, 300, 400, 500, 1500$ via a maximum penalized likelihood algorithm. Right panel: Densities predicted from the Fokker-Planck equation at the same times; scaling of the time unit used the value of $\ln \Lambda$ given in Table 1. Lower dashed curves show the density at $t = 0$; upper dashed curves show $\rho \propto r^{-7/4}$, the asymptotic solution to the Fokker-Planck equation.

correspondence between N -body and Fokker-Planck results is again quite good; the only systematic difference appears at very small radii ($r \lesssim 0.01r_h$) where the particle numbers are too small for reliable estimates of ρ . The final cusp is well represented by $\rho \propto r^{-1.75}$ at $r \lesssim 0.1r_h$, both in Run 1 and in the other integrations (not illustrated here).

The large number of particles in our N -body experiments

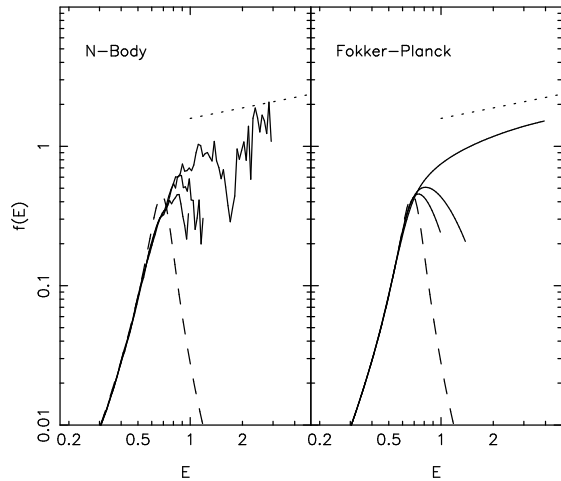


FIG. 3.— Evolution of the phase-space density of stars around the black hole in Run 5. Left panel: N -body; $f(E)$ was estimated from the particle energies at times $t = 180, 300, 600$ as described in the text. Right panel: Densities predicted from the Fokker-Planck equation at the same times; scaling of the time unit used the value of $\ln \Lambda$ given in Table 1. Lower dashed curves show $f(E)$ at $t = 0$; upper dashed curves show $f \propto E^{1/4}$, the asymptotic solution to the Fokker-Planck equation.

permits us to go one step deeper in comparing N -body with Fokker-Planck results. It is possible to extract estimates of $f(E)$ from the N -body data sets. We did this as follows. Snapshots of the particle positions and velocities were stored at each N -body time unit; such data sets are essentially uncorrelated at radii near r_h . Roughly 70 of these snapshots were then combined into a single data file, giving an effective N of $\sim 10^7$. From the combined data set we computed an estimate of the gravitational potential using standard expressions, then computed the phase-space volume element $p(E)$ defined above. The particle energies were also computed, and a histogram constructed of $N(E)$. Finally, we used the relation $f(E) = N(E)/4\pi^2 p(E)$ to compute an estimate of the phase-space density, assuming an isotropic distribution of particle velocities.

Figure 3 shows the results for Run 5 ($N = 1.5 \times 10^5$, $\gamma = 0.5$). While $f(E)$ is clearly harder to estimate than $\rho(r)$ – it is effectively a $3/2$ derivative of ρ and hence noisy – we can see from Figure 3 that the f extracted from the N -body runs evolves in a very similar way to the f computed via the Fokker-Planck equation, and that its steady-state form is consistent (modulo the noise) with the Bahcall-Wolf solution $f \propto E^{1/4}$ at late times.

6. DISCUSSION

Our results contribute to the growing body of literature demonstrating the feasibility of direct-force N -body techniques for simulating the evolution of dense stellar systems on collisional time scales. Two landmark studies in this vein were the recovery of gravothermal oscillations using the GRAPE-4 special purpose computer by Makino (1996), and the computation of the parameters of core collapse by Baumgardt et al. (2003) using the GRAPE-6. Our study extends this work to the yet more difficult case of star clusters around massive singularities, in which accurate and efficient computation of the forces is particularly critical. We have shown that particle numbers accessible to a single special-purpose computer ($\lesssim 10^6$), combined with a regularization scheme for close encounters to the black hole, are sufficient to test predictions derived from a macroscopic formulation of the evolution equations, and that the two approaches indeed make consistent predictions about the formation of a cusp on relaxation time scales.

This success points the way to even more challenging N -body studies of galactic nuclei. For instance, the “loss cone” problem – the rate at which a central black hole captures or destroys stars – has so far been the almost exclusive domain of Fokker-Planck treatments. Verifying the Fokker-Planck predictions via direct N -body simulations is feasible but will require particle numbers large enough that loss-cone refilling takes place on a time scale long compared with orbital periods. This implies $N > 10^6$ (Milosavljević & Merritt 2003), currently achievable via distributed hardware (Dorband, Hemsendorf & Merritt 2003). Related problems requiring comparably large N are the long-term evolution of binary supermassive black holes, and the Brownian motion of black holes in dense nuclei.

We are indebted to Sverre Aarseth and Seppo Mikkola who were tireless in their advice and support during the coding of the chain regularization algorithm. We gratefully acknowledge useful discussions with Marc Freitag and Simon Portegies Zwart. This work was supported via grants NSF AST 02-0631, NASA NAG5-9046 and HST-AR-09519.01-A to DM, and by the German Science Foundation (DFG) via grant SFB439 at the University of Heidelberg to RS and MP. MP also acknowledges financial support from the Fundação para a Ciência e Tecnologia (FCT), Portugal, through grant SFRH/BD/3444/2000.

REFERENCES

- Aarseth, S.J., 1999, *PASP*, 111, 1333
Aarseth, S.J. 2003, *Gravitational N-Body Simulations* (Cambridge: Cambridge University Press)
Amaro-Seoane, P., Freitag, R. & Spurzem, R. 2004, *MNRAS* in press, astro-ph/0401163
Bahcall, J. N. & Wolf, R. A. 1976, *ApJ*, 209, 214
Baumgardt, H., Heggie, D. C., Hut, P. & Makino, J. 2003, *MNRAS*, 341, 247
Cohn, H. 1980, *ApJ*, 242, 765
Cohn, H. & Kulsrud, R. M. 1978, *ApJ*, 226, 1087
Dehnen, W. 1993, *MNRAS*, 265, 250
Dorband, E. N., Hemsendorf, M. & Merritt, D. 2003, *J. Comp. Phys.*, 185, 484
Freitag, M. & Benz, W. 2002, *A&A*, 394, 345
Genzel, R. et al. 2003, *ApJ*, 594, 812
Kustaanheimo P., Stiefel E.L., *J. Reine Angew. Math.*, 218, 204
Lauer, T. R., Faber, S. M., Ajhar, E. A., Grillmair, C. J., & Scowen, P. A. 1998, *AJ*, 116, 2263
Makino, J. 1996, *ApJ*, 471, 796
Maoz, E. 1993, *MNRAS*, 263, 75
Marchant, A. B. & Shapiro, S. L. 1980, *ApJ*, 239, 685
Merritt, D. 1994, <http://www.rut.edu/drmmps/inverse.html>
Merritt, D. 2001, *ApJ*, 556, 245
Merritt, D. 2004, in “Coevolution of Black Holes and Galaxies,” Carnegie Observatories Astrophysics Series no. 1, ed. L. C. Ho (Cambridge: Cambridge University Press), 264.
Merritt, D. & Tremblay, B. 1994, *AJ*, 108, 514
Mikkola, S. & Aarseth, S. A. 1990, *Celestial Mechanics & Dynamical Astronomy*, 47, 375
Mikkola, S. & Aarseth, S. A. 1993, *Celestial Mechanics & Dynamical Astronomy*, 57, 439
Milosavljević, M. & Merritt, D. 2003, *ApJ*, 596, 860

Peebles, P. J. E. 1972a, *Gen. Rel. Grav.*, 3, 61

Peebles, P. J. E. 1972b, *ApJ*, 178, 371

Shapiro, S. L. & Lightman, A. P. 1976, *Nature*, 262, 743

Spitzer, L. 1987, *Dynamical Evolution of Globular Clusters*, Princeton Un.
Press

Young, P. 1980, *ApJ*, 242, 1232